J Electroceram (2006) 17:909–912
DOI 10.1007/s10832-006-9073-3

Photocatalytic WO_3/TiO_2 nanoparticles working under visible light

Seung Yong Chai · Yong Joo Kim · Wan In Lee

Received: 28 June 2005 / Revised: 3 March 2006 / Accepted: 9 May 2006

Abstract WO_3/TiO_2 was prepared by modifying the surface of TiO_2 with clusters of crystallized WO_3. Previously, we have reported that the TiO_2 covered with the monolayer of WO_3 shows greatly enhanced photocatalytic activity under UV light in decomposing VOCs. Here we report that the WO_3/TiO_2 can also be activated by visible light in the photocatalytic decomposition of gaseous 2-propanol. The structure of WO_3/TiO_2 was examined by X-ray diffraction (XRD), TEM, UV-Visible and Raman spectra. The samples with 10 mol% of WO_3 annealed at 700°C provide the optimum photocatalytic efficiency in visible range. We also suggest the mechanism for the WO_3/TiO_2 working under visible light.

Keywords Nanoparticle · Visible light · Photocatalyst · WO_3/TiO_2 · TiO_2

1 Introduction

TiO_2 has been known as the most efficient photocatalyst under UV light irradiation with its unique characteristics in band position and surface structure [1–3]. Extensive research has been conducted on the application of TiO_2 to the photocatalytic purification of water and air, as well as self-cleaning and super-hydrophilic smart materials [4–7].

Previously, we reported that by covering the surface of TiO_2 with the monolayer of WO_3 the photocatalytic activity of TiO_2 in decomposing gaseous 2-propanol was greatly enhanced under UV light [8]. When we measured the photocatalytic activity in visible range with the same sample, however, its activity was very low and not appreciably different from that of the pure TiO_2. Considering the visible-range band-gap and the high surface area of WO_3 covering the surface of TiO_2, it is rather unexpected result, but this would be rationalized by the following reasons. First, the WO_3/TiO_2 samples are only annealed at 200°C. At this temperature, the WO_3 covering the TiO_2 surface remains in amorphous, and the band gap may not be defined in this state. Second, intrinsically WO_3 itself is not an efficient photocatalyst, even though its absorption band-edge is positioned in the visible region.

Several strategies have been so far tried to obtain efficient photocatalysts with the WO_3/TiO_2 system. A few reports indicated that the WO_3-doped TiO_2 or TiO_2-WO_3 bilayers were photocatalytically effective under visible light [8–10]. In this work, we report a systematic study on the composites of WO_3/TiO_2 for the application to the photocatalyst working in visible range. Several compositions of WO_3/TiO_2 annealed at different temperatures were prepared, and the structures and the optical properties as well as their photocatalytic activities were characterized.

2 Experimental

Degussa P25 with an average particle size of 25 nm was chosen as the standard TiO_2. WO_3/TiO_2 was prepared by the incipient wetness method as described below. 1.0 g of TiO_2 nanoparticle was suspended in 50 ml of 2.5 M NH_4OH aqueous solution dissolved with a stoichiometric amount of H_2WO_4 (99%, Aldrich), and the suspension was dried in a water bath maintained at 60°C while vigorous stirring [8, 12]. With this procedure, the W precursors cover the surface of TiO_2. The dried sample was then heat-treated in air at several temperatures (200–900°C) for 2 hr.

S. Y. Chai · Y. J. Kim · W. I. Lee (✉)
Department of Chemistry, Inha University, #253, Yonghyun-dong, Nam-ku, Incheon 402-751, Korea
e-mail: wanin@inha.ac.kr; chaidragon@hanmail.net

The prepared WO_3/TiO_2 samples were tested as visible-range photocatalysts for the decomposition of 2-propanol in gas phase. For the photocatalytic measurements the aqueous colloidal suspensions containing 2.0 mg of WO_3/TiO_2 were spread as a film on a 2.5×2.5 cm^2 Pyrex glass, and subsequently dried at 50°C for 2 hr. The gas reactor system used for this photocatalytic reaction is described elsewhere [12]. The whole area of WO_3/TiO_2 film was irradiated by a 300 W Xe lamp through an UV cut-off filter (<400 nm, Oriel) and a water filter. After the evacuation of reactor, 1.6 μl of 2-propanol and 3.2 μl of water were added. In the reactor their partial pressures were 2 and 16 Torr, respectively. The total pressure of the reactor was then controlled to 700 Torr by addition of oxygen gas. After irradiation of 60 min, 0.5 mL of gas sample in the reactor was automatically picked up and sent to a gas chromatograph (Young Lin M600D) by using an autosampling valve system (Valco Instruments Inc. A60).

X-ray powder diffraction patterns for the WO_3/TiO_2 particles were obtained by using a Rigaku Multiflex diffractometer. TEM images of WO_3/TiO_2 particle were observed by Philips CM30 transmission electron microscope operated at 250 kV. The UV-visible diffuse reflectance spectra were obtained with a Perkin-Elmer Lambda 40, and the Raman spectra were recorded by a BRUKER RFS 100/S FT-Raman spectrophotometer.

3 Results and discussion

To prepare a junctioned structure between WO_3 and TiO_2, the 10 mol % WO_3-loaded TiO_2 samples were annealed at the temperature of 200–900°C. As shown in Fig. 1a, the crystal phase of WO_3 begins to form for the samples annealed at 600°C. Figure 1b indicates the XRD patterns of WO_3/TiO_2 annealed at 700°C as a function of WO_3 compositions. The crystallized WO_3 was appeared for the samples retaining more than 10 mol% of WO_3. Thus, the composition of WO_3 and the annealing temperature needs to be at least 10 mol % and 600°C, respectively, for the preparation of crystallized WO_3 on the surface of TiO_2.

The TEM images of Fig. 2 describe the 10 mol % WO_3-loaded TiO_2 nanoparticles annealed at 700 and 900°C, respectively. For the samples heat-treated at 900°C, the individual TiO_2 particles were merged to form the 50–100 nm-sized rutile particles, and the 2–3 nm-sized WO_3 clusters were uniformly dispersed over their surfaces without mutual aggregation. This suggests WO_3 has a good binding affinity toward TiO_2. For the samples annealed at 700°C, the size of TiO_2 was not appreciably changed compared with that of the original Degussa P25. However, WO_3 clusters were not identified over the entire region, as shown in Fig. 2c and d. This is not compatible with the result of XRD patterns, but

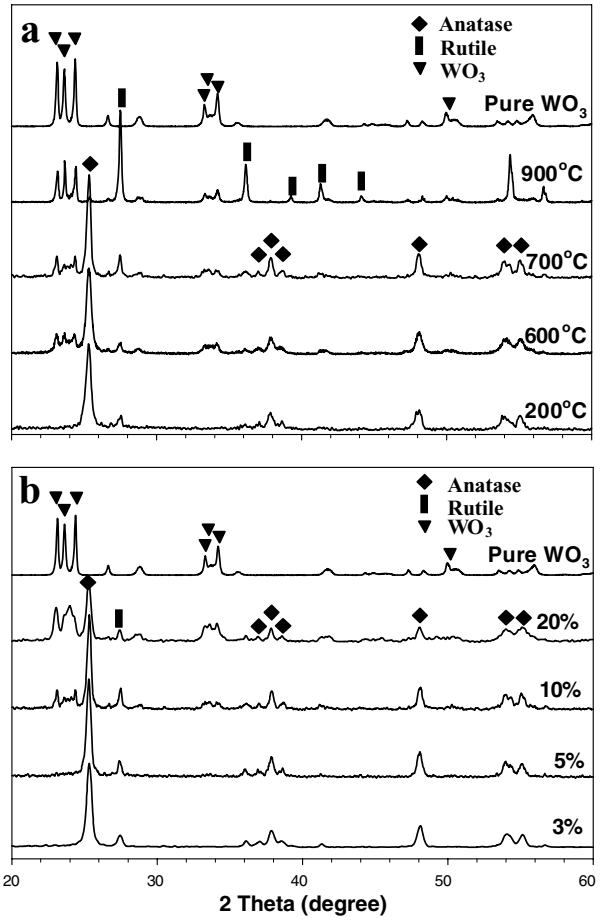

Fig. 1 XRD patterns of WO_3/TiO_2 samples. (a) 10 mol% WO_3/TiO_2 and pure WO_3 annealed at several temperatures. (b) WO_3/TiO_2 in various WO_3 compositions annealed at 700°C

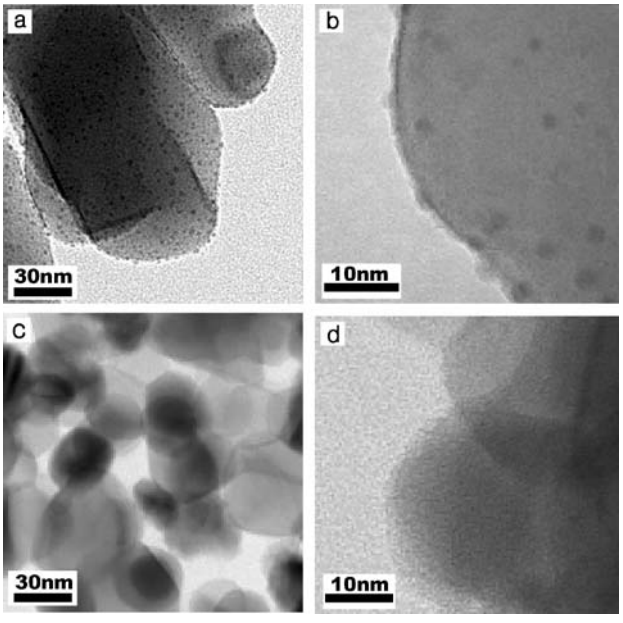

Fig. 2 TEM images for the several 10 mol% WO_3/TiO_2. (a) Annealed at 900°C. (b) Magnified image of (a). (c) Annealed at 700°C. (d) Magnified image of (c)

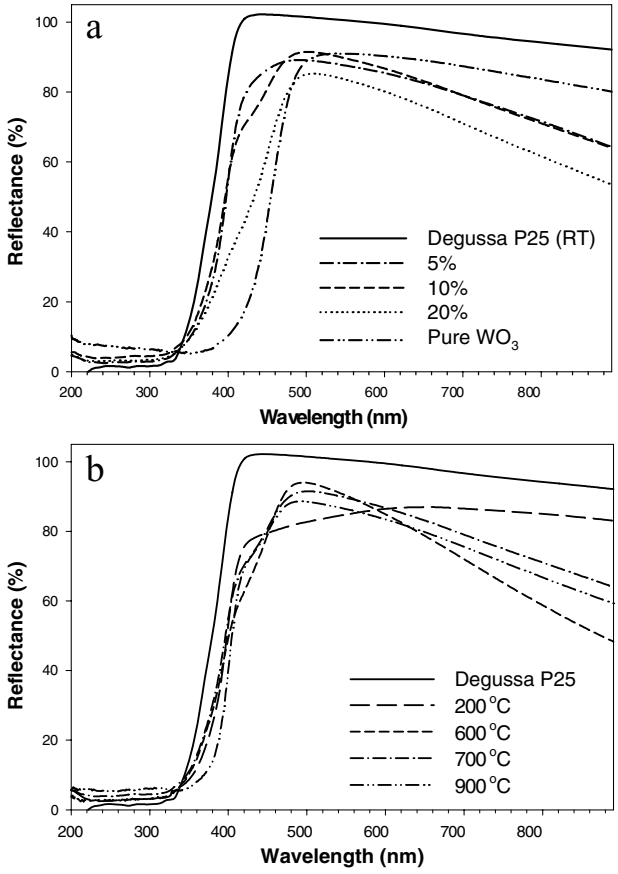

Fig. 3 Diffuse reflectance spectra of WO_3/TiO_2 in different WO_3 concentrations (a), and annealed at different temperatures (b)

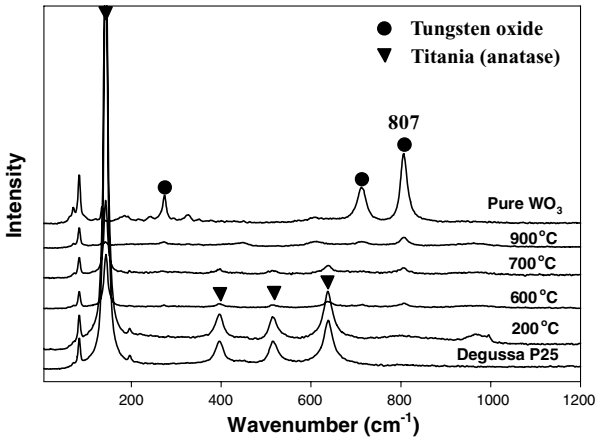

Fig. 4 Raman spectra for the 10 mol% WO_3/TiO_2 annealed at several temperatures

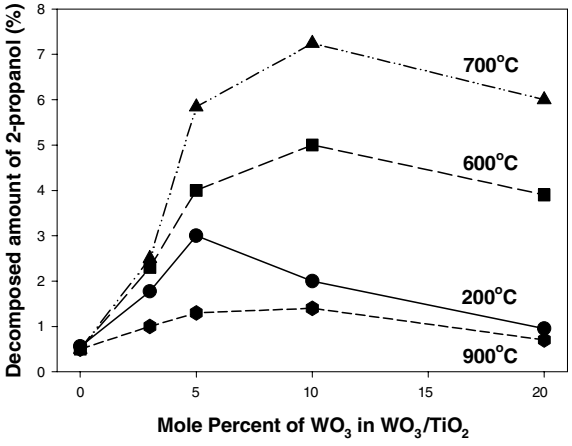

Fig. 5 Decomposition percentages of 2-propanol by the visible-light photocatalytic reaction with WO_3/TiO_2 derived at different temperature and at different mol% of WO_3. For each sample, the visible light over 400 nm was irradiated for 60 min, and the gas compositions in the reactor were 2.0 Torr of 2-propanol, 16 Torr of H_2O, and 682 Torr of O_2

we guess that the crystallite size of WO_3 clusters is tiny at this process temperature.

Figure 3 shows the diffuse reflectance spectra of WO_3/TiO_2 powders in different WO_3 concentrations and annealed at several temperatures. For the comparison, the spectra of pure TiO_2 and WO_3 powders were also included in Fig. 3a. The absorption band edge of bulk WO_3 was about 420 nm, which is red-shifted by ~80 nm from that of pure TiO_2. For the samples heat-treated at 700°C, the minimum mol% of WO_3 inducing the band-edge shift was determined to 10 mol%. Figure 3b indicates the annealing at 600°C is necessary to induce the shift of band-edge for the 10 mol% WO_3/TiO_2. Thus, the band-edge shift is caused by the formation of crystallized WO_3 phase on the surface of TiO_2. The Raman spectra for the 10 mol% WO_3/TiO_2 annealed at several temperatures were shown in Fig. 4. The peaks of 807 cm^{-1} assigned to WO_3 stretching mode begin to appear for the samples annealed at 600°C or above. This also indicates the formation temperature of crystallized WO_3 is 600°C.

We evaluated the photocatalytic activities of WO_3/TiO_2 under a visible light as a function of the concentration of WO_3 and the annealing temperature, as shown in Fig. 5. The photocatalytic activity was estimated by the decomposition% of 2-propanol in gas phase, after a 60 min of visible light irradiation. It was found that the 10 mol% WO_3/TiO_2 samples annealed at 700°C showed the highest photocatalytic efficiency in decomposing 2-propanol. Compared with pure TiO_2, it showed about 20 times of photocatalytic efficiency under a visible light.

WO_3 on TiO_2 surface begins to crystallize at 600°C, as observed from the XRD patterns and Raman spectra. With this heat-treatment, the crystallized WO_3 clusters are junctioned to TiO_2, and the resultant WO_3/TiO_2 can absorb the visible light in the wavelength over 400 nm, as described by diffuse reflectance spectra. Figure 6 describes a schematic diagram for the photocatalytic mechanism of WO_3/TiO_2 system. If the WO_3 is excited by visible light, the holes will be formed in the valence band of WO_3. Then, the electrons in the valence band of TiO_2 can move to that of WO_3. Finally, the

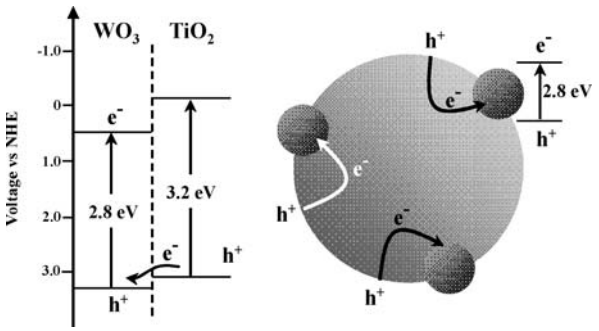

Fig. 6 Schematic diagram describing the photocatalytic mechanism in the visible light for the WO_3/TiO_2 system

holes generated in the TiO_2 can induce the photocatalytic oxidation reactions.

For the samples annealed at 900°C, the photocatalytic activity was very low, even though the WO_3 was highly crystallized. This may be caused by the formation of the large TiO_2 particles in rutile phase, and also clearly indicates WO_3 itself is not an efficient photocatalyst.

4 Conclusions

The WO_3/TiO_2 with 10 mol% of WO_3 annealed at 700°C presents 20 times of enhanced photocatalytic activity under a visible light in decomposing 2-propanol, compared with Degussa P25. With the irradiation of visible light the crystallized WO_3 clusters on the surface of TiO_2 will be excited, and subsequently the electrons in the valence band of TiO_2 can be trapped to that of WO_3. Then, the generated holes in the TiO_2 would be used for the photocatalytic oxidation reaction.

Acknowledgment This work has been supported by the Ministry of Environment, Republic of Korea (Project No. 022-061-026).

References

1. A.J. Nozik, *Annu. Rev. Phys. Chem.*, **29**, 189 (1978).
2. M.R. Hoffmann, *Chem. Rev.*, **95**, 69 (1995).
3. C.S. Turchi, and D.F. Ollis, *J. Catal.*, **122**, 178 (1990).
4. M. Miyauch, A. Nakajima, T. Watanabe, and K. Hahimoto, *Chem. Mater.*, **14**, 2812 (2002).
5. R. Wang, K. Hahimoto, A. Fujishima, M. Chikuni, E. Kojima, A. Kitamura, M. Shimohigoshi, and T. Watanabe, *Nature*, **388**, 431 (1997).
6. R. Wang, K. Hahimoto, A. Fujishima, M. Chikuni, E. Kojima, A. Kitamura, M. Shimohigoshi, and T. Watanabe, *Adv. Mater.*, **10**, 135 (1998).
7. K. Vinodgopal, U. Stafford, K.A. Gray, and P.V. Kamat, *J. Phys. Chem.*, **98**, 6797 (1994).
8. K.Y. Song, M.K. Park, Y.T. Kwon, H.W. Lee, W.J. Chung, and W.I. Lee, *Chem. Mater.*, **13**, 2349 (2001).
9. X.Z. Li, F.B. Li, C.L. Yang, and W.K. Ge, *J. Photoch. Photobio. A.*, **141**, 209, (2001).
10. T. Takahashi, H. Nakabayashi, N. Ymada, and J. Tanabe, *J. Vac. Sci. Technol. A.*, **21**, 1409 (2003).
11. M. Anpo and M. Takeuchi, *J. Catal.*, **216**, 505 (2003).
12. Y.T. Kwon, K.Y. Song, W.I. Lee, G.J. Choi, and Y.R. Do, *J. Catal.*, **191**, 192 (2000).
13. A. Fuerte, M.D. Hernandez-Alonso, A.J. Maira, A. Martinez-Arias, M. Fernandez-Garcia, J.C. Conesa, J. Soria, and G. Munuera, *J. Catal.*, **212**, 1 (2002).